THE JOURNAL OF PHYSICAL CHEMISTRY A

Article

pubs.acs.org/JPCA

Ortho–Para Mixing Hyperfine Interaction in the H_2O^+ Ion and Nuclear Spin Equilibration

Keiichi Tanaka,*[,†,‡] Kensuke Harada,[‡] and Takeshi Oka[§]

[†]Department of Applied Chemistry, National Chiao Tung University, 1001 Ta-Hsueh Rd., Hsinchu 30010, Taiwan

[‡]Department of Chemistry, Faculty of Sciences, Kyushu University, Hakozaki, Higashiku, Fukuoka 812-8581, Japan

[§]Department of Astronomy and Astrophysics and Department of Chemistry, the Enrico Fermi Institute, the University of Chicago, Chicago, Illinois 60637, United States

Supporting Information

ABSTRACT: The *ortho* to *para* conversion of water ion, H_2O^+, due to the interaction between the magnetic moments of the unpaired electron and protons has been theoretically studied to calculate the spontaneous emission lifetime between the *ortho*- and *para*-levels. The electron spin–nuclear spin interaction term, $T_{ab}(S_a\Delta I_b + S_b\Delta I_a)$ mixes *ortho* ($I = 1$) and *para* ($I = 0$) levels to cause the "forbidden" *ortho* to *para* $|\Delta I| = 1$ transition. The mixing term with $T_{ab} = 72.0$ MHz is 4 orders of magnitude higher for H_2O^+ than for its neutral counterpart H_2O where the magnetic field interacting with proton spins is by molecular rotation rather than the free electron. The resultant 10^8 increase of *ortho* to *para* conversion rate possibly makes the effect of conversion in H_2O^+ measurable in laboratories and possibly explains the anomalous *ortho* to *para* ratio recently reported by Herschel heterodyne instrument for the far-infrared (HIFI) observation.

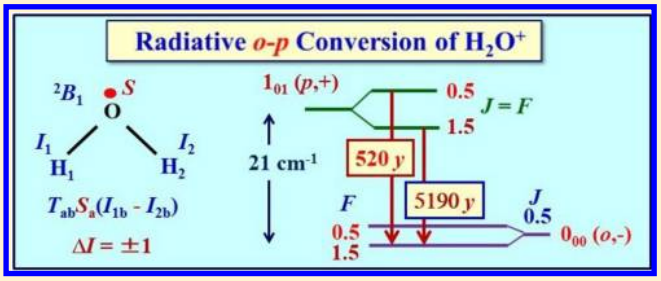

Results of our calculations show that the *ortho* ↔ *para* mixings involving near-degenerate *ortho* and *para* levels are high ($\sim 10^{-3}$), but they tend to occur at high energy levels, ~300 K. Because of the rapid spontaneous emission, such high levels are not populated in diffuse clouds unless the radiative temperature of the environment is very high. The low-lying 1_{01} (*para*) and 1_{11} (*ortho*) levels of H_2O^+ are mixed by $\sim 10^{-4}$ making the spontaneous emission lifetime for the *para* $1_{01} \rightarrow$ *ortho* 0_{00} transition 520 years and 5200 years depending on the F value of the hyperfine structure. Thus the *ortho* ↔ *para* conversion due to the unpaired electron is not likely to seriously affect thermalization of interstellar H_2O^+ unless either the radiative temperature is very high or number density of the cloud is very low.

1. INTRODUCTION

Among the selection rules of spectroscopy[1] and collision,[2] those of spin modifications such as *ortho* ↔ *ortho* and *para* ↔ *para* (equivalent to $\Delta I = 0$ where $\mathbf{I} = \mathbf{I}_1 + \mathbf{I}_2$ is the total proton spin angular momentum) are the most robust rules. Unlike the parity rule, + ↔ −, and the $\Delta J = 0, \pm 1$ rule, the $\Delta I = 0$ rule holds even for higher order interactions. This makes the conversion between *ortho* and *para* molecules extremely slow. It is so slow that the *ortho* and *para* molecules can be treated practically as different molecules in discussing thermalization of molecules.

The stability has its origin in the near-symmetry of Wigner who stated, "the special stability of *para*-H_2 is based on a symmetry property of the quantum mechanical energy operator of the hydrogen molecule; it is not only invariant when the entire set of coordinates of both protons are exchanged but also *nearly invariant* when only the Cartesian coordinates are exchanged leaving the spin coordinates unchanged".[3] The stability is the result of the smallness of the energy of the proton in the magnetic field of molecular rotation, which is on the order of $\mu_N^2/(hR^3) \approx 4$ kHz, where μ_N is the nuclear magneton and R is the interproton distance for which 1 Å is used for the order estimate. The magnetic field due to rotation of molecules is on the order of a nuclear magneton.[4] Nevertheless the symmetry of *ortho* and *para* is not rigorous, and upon scrutinizing magnetic interactions, we always find a term(s), albeit very small, that mixes the wave functions of *ortho* and *para* spin states, even for H_2.[3] Curl et al.[5] identified the mixing terms off diagonal in I that are symmetric with respect to exchanges of Cartesian *and* spin coordinates but is antisymmetric with respect to Cartesian *or* spin coordinate alone and founded the theory of nuclear spin conversion by collisions. Readers are referred to sections 3.1.3 and 3.3.3 of ref 6 for Wigner's near-symmetry and nuclear spin modifications, respectively.

Because of the robustness of the $\Delta I = 0$ rule for ordinary molecules with paired electrons, observations of spectroscopic

Special Issue: Oka Festschrift: Celebrating 45 Years of Astrochemistry

Received: December 13, 2012
Revised: March 26, 2013
Published: March 26, 2013

   dx.doi.org/10.1021/jp312270u | J. Phys. Chem. A 2013, 117, 9584–9592

transitions between different spin modifications such as *ortho* ↔ *para* ($\Delta I = 1$) have been limited to spherical tops like CH_4[7] and SF_6[8] where the two levels are very nearly degenerate. For collisions, very slow conversion between different spin modifications have been reported for CH_3F,[9] H_2CO,[10] and H_2CCH_2.[11] Clearly such slow conversion is not likely to be relevant for discussing thermalization of interstellar molecules.

This situation changes drastically for a molecule with an unpaired electron such as free radicals and radical ions like H_2O^+, which is the subject of this paper. In such molecules the protons are in the strong magnetic field of the unpaired electron, and their magnetic energy is higher by orders of magnitude. For H_2O^+, the off-diagonal electron spin−nuclear spin interaction constant is 72.0 MHz (see section 2), 4 orders of magnitude higher than that for the nuclear spin−rotation interaction of ordinary molecule like H_2O. The ratio of the Bohr magneton to the nuclear magneton provides a factor of 2000, and the ratio of the g factor of electron to the rotational magnetic moment provides a factor of ∼5. This makes the probability of *ortho* ↔ *para* conversion higher by 8 orders of magnitude and competitive with other molecular processes.

To date, the laboratory spectroscopic studies of vinyl radical H_2CCH[12,13] and its deuterated species[13−15] have been the only observed *ortho* ↔ *para* interaction for free radicals. Although the direct *ortho* ↔ *para* transitions have not been observed, large energy shifts (∼1.5 MHz) due to the $\Delta I = 1$ interaction were measured. From the observed shifts, large mixings of 0.097% and 0.0123% were calculated, and the coefficients of the mixing terms (off-diagonal Fermi contact interaction constants, δa_F) have been determined to be 68.06(53) MHz and 10.63(94) MHz for H_2CCD[14] and D_2CCD,[15] respectively. Very large rates for *ortho* ↔ *para* conversion of H_2CCH and its dueterated species by collision have been predicted.[13]

In the present paper, we will calculate the *ortho* ↔ *para* mixing in water cation, H_2O^+, and the probability of the resultant *para* → *ortho* spontaneous emission. This molecular ion, initially identified by the visible emission spectrum from Comet Kohoutek[16] based on the laboratory spectrum of Lew,[17] has recently been observed in the far-infrared in absorption by many groups using the Herschel heterodyne instrument for the far-infrared (HIFI) and quickly became a powerful probe of water chemistry and cosmic rays.[18−22] We are motivated to help understand the anomalously high *ortho* to *para* ratio of 4.8 reported by Schilke et al.[21] The formalism and calculation developed in this paper will be applicable to any other paramagnetic molecules and ions with two equivalent protons with C_{2v} symmetry, such as NH_2, CH_2^+, SH_2^+, CH_2CN, etc.

Out of the two mechanisms that cause *para* ↔ *ortho* conversion, that is, the radiative effect (spontaneous emission) and the collisional effect, the latter is irrelevant for interstellar H_2O^+ since the most abundant collision partners in space, H_2 and H, both lead to chemical collisions rather than the physical collisions. The reaction $H_2O^+ + H_2 \rightarrow H_3O^+ + H$ destroys H_2O^+, and the reaction $H_2O^+ + H \rightarrow H_2O^+ + H$ exchanges protons of H_2O^+ and H and hence converts *ortho* and *para* H_2O^+. They both have a rapid Langevin rate. Actually the latter reaction competes with the spontaneous emission calculated in this work as discussed later in section 5 of this paper.

2. *ORTHO*−*PARA* MIXING HYPERFINE INTERACTION IN THE H_2O^+ ION

The H_2O^+ ion has two equivalent protons with $I = 1/2$ (fermion). Their nuclear spin angular momenta couple with each other to give a resultant total nuclear spin angular momentum $\mathbf{I} = \mathbf{I}_1 + \mathbf{I}_2$ with eigenvalues of $I = 1$ or 0. The $I = 1$ (*ortho*) and $I = 0$ (*para*) nuclear spin functions are, respectively, symmetric and antisymmetric with respect to the permutation of the two protons. According to Pauli's exclusion principle as formulated by Heisenberg[23] and Dirac,[24] the total wave function $\psi_{total} = \psi_e\psi_v\psi_r\psi_{ns}$ changes sign upon an exchange of two fermions. Thus the symmetric *ortho* ($I = 1$) nuclear spin functions, ψ_{ns}, are combined with symmetric rotational wave function ψ_r with *even* $K_a + K_c$, and the antisymmetric *para* ($I = 0$) nuclear spin function is combined with antisymmetric rotational wave function of *odd* $K_a + K_c$ for H_2O^+ whose electronic wave function ψ_e in the ground state has the antisymmetric B_1 symmetry.[17] This is opposite to the case of H_2O whose electronic wave function in the ground state is totally symmetric A_1. Readers are referred to Tomonaga[25] for theoretical basis for Pauli's exclusion principle and its application to *ortho* and *para* H_2.

Unlike the *ortho* and *para* symmetry, the parity of a rotational level is rigorous for an isolated molecule, and it is useful to identify which *ortho* and *para* levels are mixed. Parities of the rotational levels of H_2O^+ are given by $(-1)^{K_c}$.[26] Therefore the parity rules + ↔ + and − ↔ − give ΔK_c = even.

The magnetic moment of the unpaired electron and the protons interact through two physical effects. The first is the isotropic Fermi contact interaction

$$H_F = a_F \mathbf{S}\cdot\mathbf{I} \tag{1}$$

with $a_F = (8\pi/3)\mu_e\mu_p\langle\delta(r)\rangle$, where μ_e and μ_p are the spin magnetic moments of the unpaired electron and the proton, respectively, and $\langle\delta(r)\rangle$ with the Dirac delta function $\delta(r)$ is the probability of the unpaired electron at the position of the nuclear spin. This term is diagonal in S and I and although it contributes to the hyperfine shift of the spectrum, it does not mix *ortho* and *para* levels.

The second is the anisotropic magnetic electron dipole−proton dipole interaction

$$H_{DD} = \mathbf{S}\mathbf{T}^{(1)}\mathbf{I}_1 + \mathbf{S}\mathbf{T}^{(2)}\mathbf{I}_2 = \sum_{n=1,2}\sum_{\alpha,n\beta} S_\alpha T^{(n)}_{\alpha,n\beta} I_{n\beta} \tag{2}$$

where α and β run over the molecule fixed Cartesian coordinate a, b, and c whose axes are chosen to be in the order of the smallest to the largest moment of inertia as shown in Figure 1. The components of the tensor $\mathbf{T}$ are given as

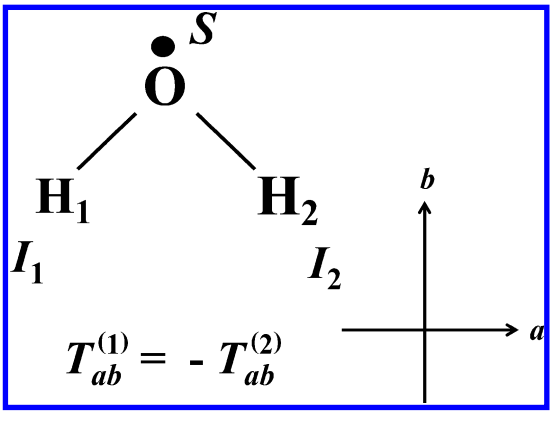

Figure 1. Molecule fixed axes in H_2O^+.

dx.doi.org/10.1021/jp312270u | J. Phys. Chem. A 2013, 117, 9584−9592

$$T^{(n)}_{\alpha\beta} = \mu_e\mu_p\langle(3\alpha\beta - r^2\delta_{\alpha\beta})/r^5\rangle \quad (3)$$

The permutation of proton 1 and proton 2, that is, the exchange of their Cartesian coordinates and spin coordinates, is a rigorous symmetry operation, which should leave the Hamiltonian invariant. This requirement is used to drop and relate some tensor components $T^{(n)}_{\alpha,n\beta}$.

From the invariance of H_{DD} for the $1 \leftrightarrow 2$ and σ_h $(c \leftrightarrow -c)$ operation, we have $T^{(1)}_{\alpha,1\alpha} = T^{(2)}_{\alpha,2\alpha} \equiv T_{\alpha\alpha}$ $(\alpha = a, b, c)$ and $T^{(n)}_{c,na} = T^{(n)}_{c,nb} = T^{(n)}_{a,nc} = T^{(n)}_{b,nc} = 0$ $(n = 1, 2)$. The invariance for the $1 \leftrightarrow 2$ and $C_2(b)$ $(a \leftrightarrow -a, c \leftrightarrow -c)$ operation gives $T^{(1)}_{a,1b} = -T^{(2)}_{a,2b} \equiv T_{ab}$ and $T^{(1)}_{b,1a} = -T^{(2)}_{b,2a} \equiv T_{ba}$. Thus the dipole–dipole interaction term is separated in to two terms $H_{DD} = H_0 + H_1$ where

$$H_0 = T_{aa}S_aI_a + T_{bb}S_bI_b + T_{cc}S_cI_c \quad (4)$$

$$H_1 = T_{ab}S_a(I_{1b} - I_{2b}) + T_{ba}S_b(I_{1a} - I_{2a}) = T_{ab}(S_a\Delta I_b + S_b\Delta I_a) \quad (5)$$

In deriving the final form of eq 5, $T_{ab} = T_{ba}$ from eq 3 is used. H_0 is diagonal in S and I like H_F, and although it shifts hyperfine levels, it does not mix *ortho* and *para* levels. H_1 is invariant with respect to the exchange of Cartesian *and* spin coordinates but changes sign with respect to the exchange of Cartesian *or* spin coordinates. Smallness of this term is the origin of Wigner's near-symmetry and the stability of the *ortho* and *para* spin modifications. This term is off-diagonal in I and mixes *ortho* and *para* levels. The selection rule of the mixing for rotational wave functions is c-type ΔK_a = odd and ΔK_c = even because the mixing Hamiltonian H_1 contains S_aI_b and S_bI_a.

In order to calculate the matrix elements of the mixing term H_1, we use Hund's case-$(b)_\beta$ basis functions $|N,K_a,S,J,I,F,M_F\rangle$ with the coupling scheme of $\mathbf{J} = \mathbf{N} + \mathbf{S}$ and $\mathbf{F} = \mathbf{J} + \mathbf{I}$. The matrix elements are diagonal with respect to S, F, and M_F but off-diagonal with respect to I (I = 1 and 0),

$$\begin{aligned}\langle N', K_a', S, J', I', F, M_F|H_1|N, K_a, S, J, I, F, M_F\rangle &= -(-1)^{I'+F+J}(30S(S+1)(2S+1)(2N+1)\\ &\quad\times(2N'+1)(2J+1)(2J'+1))^{1/2}\\ &\quad\times\langle I'\|\Delta I^{(1)}\|I\rangle\begin{Bmatrix} J' & I' & F\\ I & J & 1\end{Bmatrix}\begin{Bmatrix} N' & S & J'\\ N & S & J\\ 2 & 1 & 1\end{Bmatrix}\\ &\quad\times\sum_{p=\pm1}(-1)^{N'-K_a'}\begin{pmatrix} N' & 2 & N\\ -K_a' & p & K_a\end{pmatrix}T^{(2)}_p\end{aligned} \quad (6)$$

where $T^{(2)}_{\pm1}$ are the coefficients defined by

$$T^{(2)}_{\pm1} = \mp\frac{1}{\sqrt{6}}T_{ab} \quad (7)$$

and $\langle I'\|\Delta I^{(1)}\|I\rangle$ is the reduced matrix element of the vector $\Delta\mathbf{I} = \mathbf{I}_1 - \mathbf{I}_2$, which is $\sqrt{3}$ when I = 1 and 0. A derivation of eq 6 is given in Appendix.

Clearly the most crucial molecular parameter for calculating the *ortho–para* mixing is the off-diagonal tensor component T_{ab}. There is no experimental determination of this parameter except for NH_2, isoelectronic to H_2O^+, for which this constant has been determined by comparing the magnetic hyperfine effect of NH_2 and NHD where the molecule–fixed axis is tilted as a result of the partial deuteration. They reported $T_{ab} = 58.5 \pm 2.5$ MHz.[27] There are several theoretical papers that calculated the magnetic tensor components of H_2O^+,[28−32] but Staikova et al.[30] is the only one that gives the off-diagonal tensor component T_{ab} = 72.0 MHz (this is read from Figure 4 of the ref 30 at ∠HOH of 108.9°). The agreement between the diagonal hyperfine parameters a_F = −81.0 MHz, T_{aa} = 39.8 MHz, and T_{bb} = −14.8 MHz predicted by them and the experimental values by Mürtz et al.[33] of a_F = −75.13(27) MHz, T_{aa} = 38.91(86) MHz, and T_{bb} = −18.00(80) MHz gives an idea on the uncertainty of the theoretically calculated T_{ab} value, which is probably accurate to within 20%.

3. *ORTHO–PARA* MIXING CHANNELS IN H_2O^+

The magnitude of the mixing of wave functions of *ortho* and *para* rotational levels by H_1 is given by $\langle R_o|H_1|R_p\rangle/\Delta E_R \equiv \rho_{R_o,R_p}$, where the numerator is a shorthand for the off-diagonal matrix element of eq 5 and the denominator is the difference of energy between the mixed *ortho* and *para* levels $\Delta E_R = E_{R_o} - E_{R_p}$. In the following, we will use ρ for the cases when the mixed levels R_o and R_p are obvious and specify them only when they are needed. The *ortho* ↔ *para* conversion, which is proportional to ρ^2, is large if the two mixed levels are accidentally near-degenerate and conversion funnels through such pair of levels.[5] We have searched for the *ortho–para* mixing channels using the molecular constants reported by far-infrared laser magnetic resonance (FIR-LMR) spectroscopy.[33] In order to have nonvanishing mixing elements, the two levels must have the same F values and parities. The connection should obey the c-type selection rules in general, but significant connections are mostly between levels with ΔN = 0 or ±1, and ΔK_a = ± 1.

Because of the large rotational constants of H_2O^+, there are only several cases of near-degeneracy for rotational levels below 900 cm^{-1} as shown in Figure 2. The largest *ortho–para* mixing occurs between the $4_{22}(o)$ and $3_{30}(p)$ levels located 290 cm^{-1} above the ground state as shown in Figure 3. Due to their near-degeneracy, ΔE_R = 0.444 cm^{-1}, wave functions for F = 2.5 hyperfine components are mixed by $|\rho| = 1.17 \times 10^{-3}$. Mixing coefficients for F = 4.5 and 3.5 pairs of levels ($|\rho| = 2.7 \times 10^{-4}$ and 2.2×10^{-4}) are smaller than that for F = 2.5, because of their larger separations, ΔR = 1.136 and 2.330 cm^{-1}, respectively. Due to this interaction, the F = 2.5 and 3.5 hyperfine components of the $3_{30}(p)$ level are shifted (δE) by 18.7 and −6.0 kHz, respectively. Another large mixing channel is the $6_{51}(o)$ and $7_{43}(p)$ levels located at 880 cm^{-1} above the ground level. One of their hyperfine levels (F = 6.5) is nearly degenerate with ΔE_R = 0.335 cm^{-1} and is mixed by $|\rho| = 1.55 \times 10^{-3}$.

In the ordinary diffuse interstellar medium with number density $n \approx 10^2$ cm^{-3}, the ground *ortho* level 0_{00} and the lowest *para* level 1_{01} of H_2O^+ are the only levels that are significantly populated. Absorption from these levels, $1_{11} \leftarrow 0_{00}$ and $1_{10} \leftarrow 1_{01}$, have been observed by the Herschel HIFI.[18−22] Therefore the most interesting outcome of the *ortho–para* mixing is the $1_{01}(o) \rightarrow 0_{00}(p)$ spontaneous emission. This is discussed in the following, although there is no accidental near-degeneracy of levels involved in this case.

The low-lying $1_{01}(p)$ and $1_{11}(o)$ rotational levels, located 21 cm^{-1} above the ground $0_{00}(o)$ level, are separated by 16 cm^{-1} and split into fine and hyperfine components, F = 0.5, 1.5 and 0.5, 1.5, 2.5, respectively, as shown in Figure 4. Due to the *ortho–para* mixing hyperfine interaction, the F = 0.5 hyperfine components of the two levels are mixed by $|\rho| = 0.88 \times 10^{-4}$ and the F = 1.5 components are mixed by $(0.2–0.3) \times 10^{-4}$. These pairs of levels have relatively large matrix elements of H_1

dx.doi.org/10.1021/jp312270u | J. Phys. Chem. A 2013, 117, 9584−9592

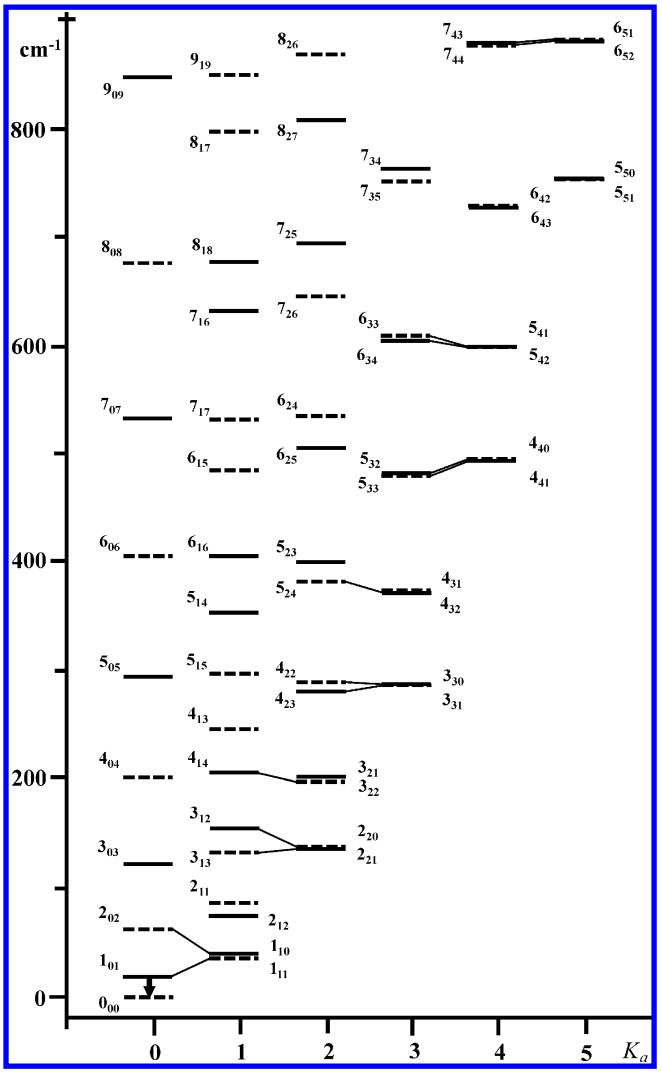

Figure 2. Rotational energy level diagram of H_2O^+ in the ground state with B_1 symmetry. *Ortho* levels, (*ee*) and (*oo*), are shown by dashed lines, while *para* levels, (*eo*) and (*oe*), are shown by solid lines. *Ortho*–*para* conversion channels due to the off-diagonal magnetic dipolar interaction with coefficient T_{ab} are shown by thin lines.

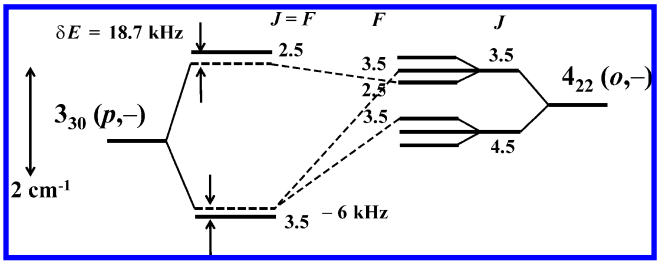

Figure 3. The 3_{30} (*p*,−) and 4_{22} (*o*,−) rotational levels split into fine and hyperfine components (splittings are exaggerated in scale for clarity) and components with the same F are mutually mixed by the *ortho*–*para* mixing dipolar interaction shown by dashed lines. The *ortho*–*para* hyperfine components (F = 2.5) are separated by 0.444 cm^{-1} and mixed by $|\rho| = 1.17 \times 10^{-3}$. As a result of this mixing, the 3_{30} level with F = 2.5 is shifted up by 18.7 kHz, while the 4_{44} level with F = 2.5 is shifted down by the same amount. The F = 3.5 component of 3_{30} level mixes with two F = 3.5 components of 4_{22} and is pushed down by 6 kHz.

thanks to the small rotational quantum number N = 1, but $|\rho|$ is small because of the large energy separation.

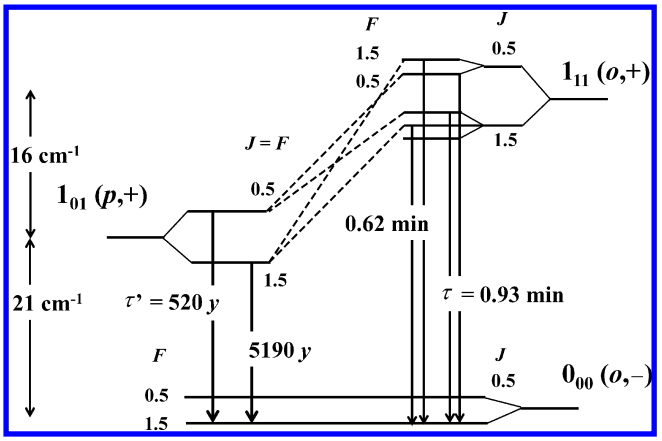

Figure 4. The 1_{01} (*p*,+) and 1_{11} (*o*,+) rotational levels split into fine and hyperfine components (splittings are exaggerated in scale) and mutually mixed by the *ortho*–*para* mixing dipolar interaction shown by dashed lines. The forbidden *para* to *ortho* converting spontaneous emissions, 1_{01} (*p*,+) → 0_{00} (*o*,−), with F = 0.5 and 1.5 occur borrowing intensities from the allowed 1_{11} (*o*,+) → 0_{00} (*o*,−) spontaneous emissions. The latter have a short lifetime of less than 1 min, while the forbidden transitions take 520 years and 5190 years for F = 0.5 → 1.5 and 1.5 → 1.5, respectively. There are other slower transitions for both allowed and forbidden transitions, which are not shown in this figure for clarity. See Table 3.

The pair of rotational levels $1_{10}(p)$ and $2_{02}(o)$, located 42 cm^{-1} above the ground level, is another example of relatively low-lying *ortho*–*para* mixing levels. The *ortho*–*para* mixing levels below 900 cm^{-1} are listed in Table 1 with their mixing $|\rho|$ and calculated frequency shifts δE due to the interaction. Unlike for CH_2CD, the shifts are very small and probably hard to observe with the present accuracy of laboratory spectroscopy.

In Table 1, we see some trends as N increases. In the high N region, the N_{0N} and N_{1N} levels with different I and the same parity are nearly degenerate. For instance, the F = 8.5 components of $9_{19}(o)$ and $9_{09}(p)$ levels are separated only by 0.0604 cm^{-1} (Figure 2). But their mixing ratio does not increase since the mixing matrix element decreases more rapidly than the energy separation.[5] Note that in low N and K_a region, the *ortho*–*para* mixing often occurs among more than two levels. This is because of the mixing ($\Delta K_a = \pm 2$) due to the asymmetry of the molecule and ($\Delta N = \pm 2$) due to the dipole hyperfine interaction H_{DD}. In such a case, root of the sum of squares of the mixing coefficients, $|\rho| = [\sum_i(\alpha_{o/p,i})^2]^{1/2}$, where $\alpha_{o/p,i}$ are the coefficients of *ortho*–*para* mixing wavefuctions in case-$(b)_\beta$ bases, is shown in the last column of Table 1.

For comparison, we tried to find the *ortho*–*para* mixing levels for NH_2 and PH_2, isoelectronic to H_2O^+, but no effective mixing levels as $4_{22}(o)$ and $3_{30}(p)$ of H_2O^+ are found for the lack of accidental degeneracy of these radicals.

4. *ORTHO*–*PARA* CONVERTING SPONTANEOUS EMISSION OF H_2O^+

The H_2O^+ ion produced in high rovibrational levels by exothermic chemical reactions will be cooled rapidly to lower levels by successive spontaneous emissions. Because of the large permanent dipole moment along the $C_2(b)$ axis, which was theoretically calculated to be 2.37 D,[29] and the large energy spacings, spontaneous emission of H_2O^+ is very fast. The

dx.doi.org/10.1021/jp312270u | J. Phys. Chem. A 2013, 117, 9584−9592

Table 1. *Ortho*−*Para* Mixing Hyperfine Interaction in H_2O^+

$N_{K_aK_c}$	o/p	J	F	E^a	ΔE^b	δE^c	$\lvert\rho\rvert^d$ (10^{-4})
				$1_{11}(o) \leftrightarrow 1_{01}(p)$ (+)			
1_{01}	(p)	0.5	0.5	20.9417	*	−4.2	0.88
1_{11}	(o)	1.5	0.5	37.2011	16.2594	0.5	0.31
1_{11}	(o)	0.5	0.5	38.0135	17.0718	3.4	0.81
1_{01}	(p)	1.5	1.5	20.8569	*	−1.2	0.32
1_{11}	(o)	1.5	1.5	37.1999	16.3431	0.1	0.20
1_{11}	(o)	0.5	1.5	38.0142	17.1573	0.1	0.21
				$2_{02}(o) \leftrightarrow 1_{10}(p)$ (−)			
1_{10}	(p)	0.5	0.5	42.0140	*	−3.7	0.77
2_{02}	(o)	1.5	0.5	62.0915	20.0775	3.6	0.77
1_{10}	(p)	1.5	1.5	41.1118	*	−2.0	0.53
2_{02}	(o)	2.5	1.5	61.9554	20.8436	0.2	0.29
2_{02}	(o)	1.5	1.5	62.0927	20.9809	0.9	0.57
				$2_{21}(p) \leftrightarrow 3_{13}(o)$ (+)			
3_{13}	(o)	2.5	1.5	131.8898	*	−1.9	1.24
2_{21}	(p)	1.5	1.5	137.5072	5.6173	3.3	1.26
3_{13}	(o)	3.5	2.5	131.4901	−0.4010	−0.8	0.82
3_{13}	(o)	2.5	2.5	131.8910	*	−2.8	1.59
2_{21}	(p)	2.5	2.5	135.6818	3.7908	3.5	1.77
				$4_{14}(p) \leftrightarrow 3_{22}(o)$ (−)			
3_{22}	(o)	3.5	3.5	198.4759	−1.4171	−1.8	0.85
3_{22}	(o)	2.5	3.5	199.8930	*	−1.6	0.90
4_{14}	(p)	3.5	3.5	206.3485	5.4555	3.6	1.25
				$3_{31}(o) \leftrightarrow 4_{23}(p)$ (+)			
4_{23}	(p)	3.5	3.5	282.7332	*	−2.7	1.09
3_{31}	(o)	3.5	3.5	288.7173	5.9840	1.3	0.87
3_{31}	(o)	2.5	3.5	291.4895	8.7563	0.7	0.52
4_{23}	(p)	4.5	4.5	281.5468	*	−1.6	0.62
3_{31}	(o)	3.5	4.5	288.7160	7.1692	0.2	0.40
				$3_{30}(p) \leftrightarrow 4_{22}(o)$ (−)			
4_{22}	(o)	3.5	2.5	291.1086	*	−18.1	11.72
3_{30}	(p)	2.5	2.5	291.5521	0.4435	18.7	11.72
3_{30}	(p)	3.5	3.5	288.7802	*	−6.0	3.50
4_{22}	(o)	4.5	3.5	289.9162	1.1359	2.5	2.72
4_{22}	(o)	3.5	3.5	291.1097	2.3295	3.3	2.20
				$5_{24}(o) \leftrightarrow 4_{32}(p)$ (−)			
4_{32}	(p)	3.5	3.5	375.8886	*	−1.0	0.65
5_{24}	(o)	4.5	3.5	385.4568	9.5682	1.4	0.64
4_{32}	(p)	4.5	4.5	373.6251	*	−1.6	0.66
5_{24}	(o)	5.5	4.5	384.3877	10.7626	0.4	0.38
5_{24}	(o)	4.5	4.5	385.4580	11.8330	1.0	0.55
				$6_{34}(p) \leftrightarrow 5_{42}(o)$ (−)			
5_{42}	(o)	5.5	5.5	601.9135	−3.1131	−1.6	0.90
5_{42}	(o)	4.5	5.5	605.0266	*	−2.0	1.42
6_{34}	(p)	5.5	5.5	608.3539	3.3273	3.4	1.69
				$6_{33}(o) \leftrightarrow 5_{41}(p)$ (+)			
5_{41}	(p)	4.5	4.5	605.0730	*	−0.9	0.66
6_{33}	(o)	5.5	4.5	612.9422	7.8691	1.1	0.65
5_{41}	(p)	5.5	5.5	601.9608	*	−1.4	0.66
6_{33}	(o)	6.5	5.5	611.1792	9.2184	0.4	0.40
6_{33}	(o)	5.5	5.5	612.9434	10.9826	0.9	0.53
				$6_{52}(p) \leftrightarrow 7_{44}(o)$ (−)			
7_{44}	(o)	6.5	5.5	880.6016	*	−1.1	0.90
6_{52}	(p)	5.5	5.5	885.6350	5.0333	1.3	0.90
7_{44}	(o)	7.5	6.5	878.1076	−2.4952	−0.9	0.93
7_{44}	(o)	6.5	6.5	880.6027	*	−7.3	4.67
6_{52}	(p)	6.5	6.5	881.7157	1.1130	8.1	4.76
				$6_{51}(o) \leftrightarrow 7_{43}(p)$ (+)			
7_{43}	(p)	6.5	6.5	881.3853	*	−25.4	15.52
6_{51}	(o)	6.5	6.5	881.7205	0.3351	24.1	15.50
6_{51}	(o)	5.5	6.5	885.6403	4.2550	1.2	0.98

[a]Energy of the hyperfine component of the rotational level in cm^{-1}. Note that for 0_{00}, $E = -0.00125$ cm^{-1} ($F = 1.5$) and 0.00251 cm^{-1} ($F = 0.5$). [b]Energy difference from the level specified with * in cm^{-1}. [c]Level shift caused by the T_{ab} term in kHz. [d]Mixing of wavefuctions for the *ortho* and *para* levels. When mixing occurs among more than two levels, a square root of the sum of squares is shown.

dx.doi.org/10.1021/jp312270u | J. Phys. Chem. A 2013, 117, 9584−9592

emission occurs between levels with the same total nuclear spin quantum number ($\Delta I = 0$) and opposite parities (ΔK_c = odd), obeying the *b*-type selection rules ($\Delta N = 0$ or ± 1,ΔK_a = odd, ΔK_c = odd). The Einstein A_{if} coefficient for the spontaneous emission[34] is given by

$$A_{if} = \frac{64\pi^4 \nu_{ij}^{\ 3}}{3c^3 h} |\mu_{if}|^2 \tag{8}$$

This gives very short lifetime; for example, the lifetime for the spontaneous emission $1_{11} \rightarrow 0_{00}$ is less than 1 min (Figure 4) and that for the $3_{30} \rightarrow 2_{21}$ emission is less than 1 s.

Weak forbidden *ortho*−*para* transitions occur borrowing intensities from the strong $\Delta I = 0$ allowed transitions. They follow *a*-type selection rules ($\Delta N = 0$, ± 1, and ± 2, ΔK_a = even, ΔK_c = odd) since the allowed transitions obey *b*-type selection rules and the mixing obeys *c*-type selection rules.

The probabilities of *ortho*−*para* converting spontaneous emission of H_2O^+ can be calculated by replacing μ_{if} with $\mu_{if}\ \rho$ and ν_{ij} with $\nu_{i'j}$ in eq 4 where the level i' is *ortho*−*para* mixed with level *i*. Thus the $i' \rightarrow j$ forbidden *ortho*−*para* converting spontaneous emission with frequency $\nu_{i'j}$ is slower than the $i \rightarrow j$ allowed transition by a factor of $(\nu_{i'j}/\nu_{ij})^3\rho^2$. Since ρ is on the order of 10^{-3} to 10^{-4} and $\nu_{i'j} \approx \nu_{ij}$, the forbidden transitions are slower than the allowed by a factor of 10^6 to 10^8.

For example, the lifetimes of the allowed spontaneous emission $3_{30}(p) \rightarrow 2_{21}(p)$ and the $4_{22}(o) \rightarrow 3_{13}(o)$ in the far-infrared region are less than 0.5 and 1.5 s, respectively. As discussed earlier, the $3_{30}(p)$ and $4_{22}(o)$ levels are mixed by a relatively large factor of $|\rho| = 1.17 \times 10^{-3}$ due to their near-degeneracy, $\Delta E_R = 0.444$ cm^{-1}. The forbidden $4_{22}(o) \rightarrow 2_{21}(p)$ and $3_{30}(p) \rightarrow 3_{13}(o)$ spontaneous emission due to this mixing occur with the lifetimes of 4.8−58 and 22−100 days, respectively, depending on the hyperfine components. Calculated spontaneous emissions due to this mixing are listed in Table 2.

The spontaneous emission lifetime for the $1_{11}(o) \rightarrow 0_{00}(o)$ (ν = 37 cm^{-1}) transition is 0.58−4.9 min depending on hyperfine component (Figure 4). The forbidden $1_{01}(p) \rightarrow 0_{00}(o)$ spontaneous emission at ν' = 21 cm^{-1} occurs by borrowing intensity of the allowed transition with relative intensity $(\nu'/\nu)^3 \times \rho^2 = 0.182 \times 10^{-8}$ to 10^{-10}. The spontaneous emission lifetimes thus calculated for the $1_{01}(p) \rightarrow 0_{00}(o)$ transition from the F = 0.5 and 1.5 hyperfine components of $1_{01}(p)$ to the lower components J = 0.5 and F = 1.5 of $0_{00}(o)$ are 520 and 5190 years, respectively, as listed in Table 3. The transitions from the hyperfine components of $1_{01}(p)$ to the higher component J = 0.5 and F = 0.5 of $0_{00}(o)$ are almost completely forbidden with lifetimes more than one million years because of the small mixing factors.

5. DISCUSSION

The forbidden spontaneous emissions between *ortho* and *para* levels like $4_{22}(o) \rightarrow 2_{21}(p)$ and $3_{30}(p) \rightarrow 3_{13}(o)$ with life times on the order of a week to a few months cannot compete with collisional processes in laboratory experiments since the number density is very high. In interstellar space where the number density is low, the radiative temperature is too low and spontaneous emission of allowed transitions are too fast for these high rotational levels to be populated. The only possibility to observe their effect will be in regions with high radiative temperature. Such a region has been recently found toward Herschel 36 through the observations of rotationally excited J = 1 CH^+ and fine structure excited J = 3/2 CH, but their radiative temperatures are only 14.6 and 6.7 K,[35] respectively. They are well above the temperature of the 2.73 K cosmic blackbody radiation but far below 100 K where radiative excitation to those N = 3 or 4 H_2O^+ rotational levels becomes relevant. Considering that Herschel 36 is the only sightline out of more than 200 sightlines that showed this excitation, it looks like a long shot to expect H_2O^+ in an environment with high enough radiative temperature.

This is not a problem for the $1_{01}(p) \rightarrow 0_{00}(o)$ spontaneous emission involving the lowest levels. However its calculated lifetime of τ = 520 years seems too long to be competitive with collisional processes. The reaction $H_2O^+ + H_2 \rightarrow H_3O^+ + H$, which destroys H_2O^+, has a Langevin rate constant of $k_L = \sim 10^{-9}$ cm^3 s^{-1}.[36] The critical density of the spontaneous emission is on the order of $1/\tau k_L \approx 0.1$ cm^{-3}, which is perhaps far too low for any environment where H_2O^+ abounds. The rate of the *ortho* ↔ *para* converting reaction, $H_2O^+(o/p) + H \rightarrow (H_3O^+)^* \rightarrow H_2O^+(p/o) + H$, has not been measured, but in view of high rate constants for other *ortho*−*para* converting chemical reactions such as $H_2(o/p) + H^+ \leftrightarrow H_2(p/o) + H^+$, 4.15×10^{-10} cm^3 s^{-1},[37] and $H_3^+ + H_2 \leftrightarrow H_3^+ + H_2$,[38] the slow spontaneous emission is perhaps not competitive since H_2O^+ resides in environments with much atomic hydrogen.[18−22]

In conclusion, the forbidden *ortho* ↔ *para* transition in H_2O^+ is 8 orders of magnitude faster than that in H_2O but still not fast enough to be relevant in the analysis of the observed *ortho* to *para* ratio. The present work was initiated with two goals in mind: (1) to quantify and formulate the *ortho*−*para* conversion rates in open shell molecules and (2) to help explain the reported anomalously high *ortho* to *para* ratio of 4.8 for H_2O^+.[21] It was later found, however, that the high *ortho* to *para* ratio was due to an error in the analysis and the true value is closer to 3, the common *ortho* to *para* ratio.[39] Therefore the second goal has disappeared.

Nevertheless the theoretical analysis given in this paper will provide a basis for future studies of *ortho* to *para* conversion. This reminds us of the other case of forbidden centrifugal distortion induced transition in NH_3 where the spontaneous emission with lifetimes on the order of a few hundred years was theoretically calculated in 1971.[40] The result was of little relevance then but 30 years later the same transitions became indispensable in the analysis of H_3^+[41,42] for which the lifetime of the spontaneous emission is on the order of 30 days. Unlike the case of the centrifugal effect, which is larger in lighter molecules, the interaction between the electron spin and nuclear spin is independent of the mass of the molecule. Therefore it is likely that the present formulation will some day be more useful and relevant for analyzing the *ortho*−*para* conversion in heavier open shell molecules in which the near-degeneracy between *ortho* and *para* levels is more likely to occur.

dx.doi.org/10.1021/jp312270u | J. Phys. Chem. A 2013, 117, 9584−9592

Table 2. *Ortho*–*Para* Mixing Transitions of H_2O^+ Due to the $4_{22}(o) \leftrightarrow 3_{30}(p)$ Interaction

J'	F'	J	F	ν^a	$\delta\nu^b$	A_{ij}^c	τ_{ij}^d
				$3_{30}(p) \rightarrow 2_{21}(p)^e$			
3.5	3.5	2.5	2.5	153.0984	−9.4	2.190	0.008
2.5	2.5	2.5	2.5	155.8703	15.1	0.146	0.114
2.5	2.5	1.5	1.5	154.0450	15.3	2.078	0.008
				$4_{22}(o) \rightarrow 2_{21}(p)$			
4.5	3.5	2.5	2.5	154.2343	−0.9	0.219	0.145
3.5	3.5	2.5	2.5	154.4279	−0.1	0.199	0.160
3.5	2.5	2.5	2.5	155.4268	−21.6	0.255	0.124
3.5	2.5	1.5	1.5	153.6015	−21.3	2.536	0.013
				$4_{22}(o) \rightarrow 3_{13}(o)^e$			
3.5	2.5	3.5	3.5	159.6200	−18.0	0.002	7.624
3.5	2.5	3.5	2.5	159.6186	−17.2	0.025	0.674
3.5	2.5	2.5	3.5	159.2160	−18.1	0.002	10.84
3.5	2.5	2.5	2.5	159.2176	−15.2	0.074	0.225
3.5	2.5	2.5	1.5	159.2188	−16.1	0.609	0.027
4.5	3.5	3.5	4.5	158.4294	2.8	0.001	30.64
4.5	3.5	3.5	3.5	158.4276	2.5	0.043	0.384
4.5	3.5	3.5	2.5	158.4261	3.3	0.658	0.025
3.5	3.5	3.5	4.5	159.6229	3.6	0.002	10.17
3.5	3.5	3.5	3.5	159.6211	3.3	0.024	0.708
3.5	3.5	3.5	2.5	159.6197	4.1	0.002	11.21
3.5	3.5	2.5	3.5	159.2171	3.3	0.056	0.300
3.5	3.5	2.5	2.5	159.2187	6.1	0.629	0.026
				$3_{30}(p) \rightarrow 3_{13}(o)$			
2.5	2.5	3.5	3.5	160.0635	18.6	0.003	11.57
2.5	2.5	3.5	2.5	160.0621	19.4	0.048	0.666
2.5	2.5	2.5	3.5	159.6595	18.6	0.002	16.47
2.5	2.5	2.5	2.5	159.6611	21.4	0.147	0.215
2.5	2.5	2.5	1.5	159.6623	20.5	0.542	0.058
3.5	3.5	3.5	3.5	157.2916	−5.9	0.008	4.101
3.5	3.5	3.5	2.5	157.2902	−5.1	0.110	0.289
3.5	3.5	2.5	3.5	156.8876	−5.9	0.002	12.89
				$3_{30}(p) \rightarrow 3_{13}(o)$			
3.5	3.5	2.5	2.5	156.8892	−3.1	0.163	0.194
				$3_{30}(p) \rightarrow 4_{13}(o)$			
3.5	3.5	4.5	3.5	44.1833	−6.1	0.004	9.002
3.5	3.5	3.5	3.5	43.5654	−6.3	0.002	17.650
2.5	2.5	4.5	3.5	46.9552	18.5	0.003	11.978
2.5	2.5	3.5	3.5	46.3373	18.2	0.007	4.507
2.5	2.5	3.5	2.5	46.3386	18.0	0.083	0.380
				$4_{22}(o) \rightarrow 3_{21}(p)$			
4.5	3.5	3.5	3.5	88.4205	3.3	0.011	2.900
3.5	3.5	3.5	3.5	89.6141	4.1	0.006	4.932
3.5	2.5	3.5	3.5	89.6129	−17.3	0.011	2.996
2.5	2.5	2.5	2.5	88.2161	−17.7	0.241	0.132
				$5_{33}(o) \rightarrow 3_{30}(p)$			
5.5	4.5	3.5	3.5	190.8511	5.8	0.229	0.139
4.5	4.5	3.5	3.5	192.8245	5.5	0.169	0.188
4.5	3.5	3.5	3.5	192.8234	5.8	0.020	1.569
4.5	3.5	2.5	2.5	190.0515	−18.8	3.199	0.010
				$4_{31}(o) \rightarrow 3_{30}(p)$			
4.5	4.5	3.5	3.5	85.2749	5.5	0.002	18.636
4.5	3.5	3.5	3.5	85.2760	5.9	0.015	2.092
3.5	3.5	3.5	3.5	87.5375	6.0	0.010	3.277
3.5	2.5	3.5	3.5	87.5367	6.1	0.003	10.980
4.5	3.5	2.5	2.5	82.5041	−18.6	0.006	5.243
3.5	3.5	2.5	2.5	84.7656	−18.6	0.018	1.706
3.5	2.5	2.5	2.5	84.7647	−18.5	0.277	0.115
				$4_{41}(p) \rightarrow 4_{22}(o)$			
4.5	4.5	4.5	3.5	205.7173	−2.0	0.476	0.067
4.5	4.5	3.5	3.5	204.5238	−2.8	0.342	0.092
3.5	3.5	4.5	3.5	209.3698	−1.9	0.014	2.316
3.5	3.5	3.5	3.5	208.1762	−2.7	0.008	4.106
3.5	3.5	3.5	2.5	208.1774	18.6	7.766	0.004

[a]Transition frequency in cm^{-1}. [b]Frequency shift caused by the T_{ab} term in kHz. [c]Einstein's A coefficient in $\times 10^{-6}$ s^{-1}, except for o–o and p–p transitions, which are in s^{-1}. [d]Lifetime of spontaneous emission in years, except for o–o and p–p transitions, which are in minutes. [e]Example of o–o and p–p transitions, which give the line intensities for the o–p transitions.

Table 3. *Ortho*–*Para* Mixing Transitions of H_2O^+ Due to the $1_{11}(o) \leftrightarrow 1_{01}(p)$ Interaction

J'	F'	J	F	ν^a	$\delta\nu^b$	A_{if}^c	τ_{if}^d
				$1_{11}(o),+ \rightarrow 0_{00}(o),-$			
1.5	1.5	0.5	1.5	1115.2631	0.6	1.351	1.234
1.5	1.5	0.5	0.5	1115.1504	0.0	1.672	0.997
0.5	1.5	0.5	1.5	1139.6733	0.6	1.784	0.934
0.5	1.5	0.5	0.5	1139.5606	0.1	1.441	1.156
1.5	0.5	0.5	1.5	1115.2987	1.0	0.339	4.919
1.5	0.5	0.5	0.5	1115.1860	0.4	2.683	0.621
0.5	0.5	0.5	1.5	1139.6537	3.9	2.864	0.582
0.5	0.5	0.5	1.5	1139.5401	3.3	0.361	4.611
				$1_{01}(p),+ \rightarrow 0_{00}(o),-$			
1.5	1.5	0.5	1.5	625.3104	−0.6	0.611	5 187
1.5	1.5	0.5	0.5	625.1977	−1.1	0.000	8.36×10^6
0.5	0.5	0.5	1.5	627.8529	−3.5	6.103	519.7
0.5	0.5	0.5	0.5	627.7402	−4.1	0.002	2.03×10^6

[a]Transition frequency in GHz. [b]Frequency shift caused by the T_{ab} term in kHz. [c]Einstein's A coefficient in $\times 10^{-2}$ s^{-1} or $\times 10^{-11}$ s^{-1} for o–o or o–p transitions. [d]Lifetime of spontaneous emission in minutes, except for o–p transitions, which are in years.

APPENDIX: MATRIX ELEMENTS OF H_1 WITH CASE-$(b)_\beta$ BASES

The molecule fixed components of **S** will be expanded with its space-fixed components,

$$S_z = \sqrt{\frac{8\pi^2}{3}} \sum_q (-1)^q \Psi_{1,-q,0}(\theta, \phi, \chi) S_q^{(1)},$$

$$S_x \pm iS_y = \pm\sqrt{\frac{16\pi^2}{3}} \sum_q (-1)^q \Psi_{1,-q,\mp1}(\theta, \phi, \chi) S_q^{(1)} \quad (9)$$

where $S_q^{(1)}$ are the components of a first rank tensor given by $S_0^{(1)} = S_Z$ and $S_{\pm1}^{(1)} = \mp(1/\sqrt{2})(S_X \pm iS_Y)$ with the space-fixed components of **S** and $\Psi_{J,M,K}(\theta,\varphi,\chi)$ is the rotational wavefuction of symmetric top molecule. Similarly the molecule-fixed components of **ΔI** are expanded with its space-fixed components as

dx.doi.org/10.1021/jp312270u | J. Phys. Chem. A 2013, 117, 9584–9592

$$\Delta I_z = \sqrt{\frac{8\pi^2}{3}} \sum_q (-1)^q \Psi_{1,-q,0}(\theta, \phi, \chi) \Delta I_q^{(1)},$$

$$\Delta I_x \pm i\Delta I_y = \pm\sqrt{\frac{16\pi^2}{3}} \sum_q (-1)^q \Psi_{1,-q,\mp 1}(\theta, \phi, \chi) \Delta I_q^{(1)} \tag{10}$$

where $\Delta I_q^{(1)}$ are the components of a first rank tensor $\Delta \mathbf{I}^{(1)}$ given by $\Delta I_0^{(1)} = \Delta I_Z$ and $\Delta I_{\pm 1}^{(1)} = \mp(1/\sqrt{2})(\Delta I_X \pm i\Delta I_Y)$ with the space-fixed components of $\Delta \mathbf{I}$.

The operators $(1/2)\{S_z(\Delta I_x \pm i\Delta I_y) + (S_x \pm iS_y)\Delta I_z\}$ are scalar products of first rank tensors, and the following relations are given after some manipulations,

$$\frac{1}{2}\{S_z(\Delta I_x \pm i\Delta I_y) + (S_x \pm iS_y)\Delta I_z\} = \mp\sqrt{\frac{8\pi^2}{3}} \sum_q (-1)^q U_{q,\mp 1}^{(1)} \Delta I_{-q}^{(1)} \tag{11}$$

where the components of the first rank tensor $U_{q,\mp 1}^{(1)}$ are given by

$$U_{q,\mp 1}^{(1)} = \sum_{q_1} \sum_{q_2} \langle 2, q_1, 1, q_2 | 1, q\rangle \Psi_{2,q_1,\mp 1}(\theta, \phi, \chi) S_{q_2}^{(1)} \tag{12}$$

and $\langle 2,q_1,1,q_2|1,q\rangle$ is the Clebsch−Gordan coefficient.

The matrix elements of scalar product of first rank tensors, eq 11, will be given by coupled tensor operators theory,[43]

$$\begin{aligned}&\langle N', K_a', S, J', I', F, M_F|\frac{1}{2}\{S_z(\Delta I_x \pm i\Delta I_y) + (S_x \pm iS_y)\Delta I_z\}|N, K_a, S, J, I, F, M_F\rangle \\ &= \mp\sqrt{\frac{8\pi^2}{3}}(-1)^{I'+F+J}\langle I'||\Delta I^{(1)}||I\rangle \times \langle N', K_a', S, J'||U_{\mp 1}^{(1)}||N, K_a, S, J\rangle \begin{Bmatrix} J' & I' & F \\ I & J & 1 \end{Bmatrix}\end{aligned} \tag{13}$$

The reduced matrix elements of first-rank tensors of $U_{\mp 1}^{(1)}$ will be given by

$$\begin{aligned}&\langle N', K_a', S, J'||U_{\mp 1}^{(1)}||N, K_a, S, J\rangle \\ &= \langle N', K_a'||\Psi_{\mp 1}^{(2)}||N, K_a\rangle\langle S||S^{(1)}||S\rangle \times \sqrt{3(2J+1)(2J'+1)} \begin{Bmatrix} N' & S & J' \\ N & S & J \\ 2 & 1 & 1 \end{Bmatrix}\end{aligned} \tag{14}$$

where the reduced matrix elements are given by

$$\langle S||S^{(1)}||S\rangle = \sqrt{S(S+1)(2S+1)} \tag{15}$$

$$\begin{aligned}&\langle N', K_a'||\Psi_{\mp 1}^{(2)}||N, K_a\rangle \\ &= \sqrt{\frac{5}{8\pi^2}}(-1)^{N'-K_a'}\sqrt{(2N+1)(2N'+1)} \times \begin{pmatrix} N' & 2 & N \\ -K_a' & \mp 1 & K_a \end{pmatrix}\end{aligned} \tag{16}$$

Combining eqs 13−16, we obtain for eq 13

$$\begin{aligned}&= \mp\sqrt{5}(-1)^{I'+F+J}(-1)^{N'-K_a'} \times \sqrt{(2J+1)(2J'+1)(2N+1)(2N'+1)} \\ &\times \sqrt{S(S+1)(2S+1)}\langle I'||\Delta I^{(1)}||I\rangle \times \begin{Bmatrix} J' & I' & F \\ I & J & 1 \end{Bmatrix} \\ &\times \begin{Bmatrix} N' & S & J' \\ N & S & J \\ 2 & 1 & 1 \end{Bmatrix}\begin{pmatrix} N' & 2 & N \\ -K_a' & \mp 1 & K_a \end{pmatrix}\end{aligned} \tag{17}$$

With the use of the relations

$$\begin{aligned}S_z\Delta I_x + S_x\Delta I_z &= \frac{1}{2}\{S_z(\Delta I_x + i\Delta I_y) + (S_x + iS_y)\Delta I_z\} \\ &+ \frac{1}{2}\{S_z(\Delta I_x - i\Delta I_y) + (S_x - iS_y)\Delta I_z\}\end{aligned} \tag{18}$$

and if we replace T_{ab} with $T_{\pm 1}^{(2)}$ given in eq 7, then we have matrix elements of $H_1 = T_{ab}(S_a\Delta I_b + S_b\Delta I_a)$ given in eq 6, where molecular axis system (a, b, c) corresponds to that of (z, x, y).

■ ASSOCIATED CONTENT

Supporting Information

The complete author list for refs 18−22. This information is available free of charge via the Internet at http://pubs.acs.org.

■ AUTHOR INFORMATION

Corresponding Author

*E-mail: ktanaka@chem.kyushu-univ.jp.

Notes

The authors declare no competing financial interest.

■ ACKNOWLEDGMENTS

We acknowledge Prof. Eric Herbst and Prof. Takehiko Tanaka for valuable discussions. One of the authors (K.T.) thanks National Science Council of Taiwan for the visiting professorship in National Chiao Tung University. T.O. acknowledges the support by the NSF Grant AST 1109014.

■ REFERENCES

(1) Herzberg, G. *Molecular Spectra and Molecular Structure*; Krieger Publishing Company: Malabar, FL, 1989; Vols. *I*, *II*, and *III*.
(2) Oka, T. Collision-Induced Transitions between Rotational Levels. *Adv. At. Mol. Phys.* **1973**, *9*, 127−176.
(3) Wigner, E. Über die Paramagnetische Umwandlung von Para-Orthowasserstoff. III. *Z. Phys. Chem.* **1933**, *B23*, 28−32.
(4) Townes, C. H.; Schawlow, A. L. *Microwave Spectroscopy*; McGraw-Hill Book Company Inc.: New York, 1955.
(5) Curl, R. F., Jr.; Kasper, J. V. V; Pitzer, K. S. Nuclear Spin State Equilibration through Nonmagnetic Collisions. *J. Chem. Phys.* **1967**, *46*, 3220−3228.
(6) Oka, T. Orders of Magnitude and Symmetry in Molecular Spectroscopy. *Handbook of High-resolution Spectroscopy*; Quack, M., Merkt, F., Eds.; John Wiley & Sons, Ltd: Hoboken, NJ, 2010.
(7) Ozier, I.; Yi, P N.; Khosla, A.; Ramsay, N. F. Direct Observation of Ortho-Para Transitions in Methane. *Phys. Rev. Lett.* **1970**, *24*, 642−646.
(8) Bordé, J.; Bordé, Ch. J.; Salomon, C.; Van Lerberghe, A.; Ouhayoun, M.; Cantrell, C. D. Breakdown of the Point-Group Symmetry of Vibration-Rotation States and Optical Observation of Ground-State Octahedral Splittings of $^{32}SF_6$ Using Saturation Spectroscopy. *Phys. Rev. Lett.* **1980**, *45*, 14−17.

(9) Chapovsky, P. L.; Krasnoperov, L. N.; Panfilov, V. N.; Strunin, V. P. Studies on Separation and Conversation of Spin Modification of CH_3F Molecules. *Chem. Phys.* **1985**, *97*, 449−455. Chapovsky, P. L.; Hermans, L. J. F. Nuclear Spin Conversation in Polyatomic Molecules. *Annu. Rev. Phys. Chem.* **1999**, *50*, 315−345.
(10) Peters, G.; Schramm, B. Nuclear Spin State Relaxation in Formaldehyde: Dependence of the Rate Constant on Pressure. *Chem. Phys. Lett.* **1999**, *302*, 181−186.
(11) Sun, Z.-D.; Takagi, K.; Matsushima, F. Separation and Conversion Dynamics of Four Nuclear Spin Isomers of Ethylene. *Science* **2005**, *310*, 1938−1941.
(12) Tanaka, K.; Toshimitsu, M.; Harada, K.; Tanaka, T. Determination of the Proton Tunneling Splitting of the Vinyl Radical in the Ground State by Millimeter-Wave Spectroscopy Combined with Supersonic-Jet Expansion Technique and Ultraviolet Photolysis. *J. Chem. Phys.* **2004**, *120*, 3604−3618.
(13) Tanaka, K.; Hayashi, M.; Ohtsuki, M.; Harada, K.; Tanaka, T. Millimeter-Wave Spectroscopy of Deuterated Vinyl Radicals, Observation of the *Ortho-Para* Mixing Interaction and Prediction of Fast *Ortho-Para* Conversion Rates. *Mol. Phys.* **2010**, *108*, 2289−2301.
(14) Tanaka, K.; Hayashi, M.; Ohtsuki, M.; Harada, K.; Tanaka, T. *Ortho-Para* Mixing Interaction in the Vinyl Radical Detected by Millimeter-Wave Spectroscopy. *J. Chem. Phys.* **2009**, *131*, No. 111101.
(15) Hayashi, M.; Harada, K.; Lavrich, R.; Tanaka, T.; Tanaka, K. Millimeter-Wave Spectroscopy of $H_2C{=}CD$: Tunneling Splitting and *Ortho-Para* Mixing Interaction. *J. Chem. Phys.* **2010**, *133*, No. 154303.
(16) Herzberg, G.; Lew, H. Tentative Identification of the H_2O^+ Ion in Comet Kohoutek. *Astron. Astrophys.* **1974**, *31*, 123−124.
(17) Lew, H. Electronic Spectrum of H_2O^+. *Can. J. Phys.* **1976**, *54*, 2028−2049.
(18) Gerin, M.; De Luca, M.; Black, J.; Goicoechea, J. R.; Herbst, E.; Neufeld, D. A.; Falgarone, E.; Godard, B.; Pearson, J. C.; Lis, D. C.; et al. Interstellar OH^+, H_2O^+ and H_3O^+ Along the Sight-Line to G10.6-0.4. *Astron. Astrophys.* **2010**, *518*, No. L110.
(19) Ossenkopf, V.; Müller, H. S. P.; Lis, D. C.; Schilke, P.; Bell, T. A.; Bruderer, S.; Bergin, E.; Ceccarrelli, C.; Comito, C.; Stutzki, J.; et al. Detection of Interstellar Oxidaniumyl: Abundant H_2O^+ Towards the Star-Forming Regions DR21, Sgr B2, and NGC6334. *Astron. Astrophys.* **2010**, *518*, No. L111.
(20) Neufeld, D. A.; Goicoechea, J. R.; Sonnentrucker, P.; Black, J. H.; Pearson, J.; Yu, S.; Phillips, T. G.; Lis, D. C.; De Luca, M.; Herbst, E.; et al. Herschel/HIFI Observations of Interstellar OH^+ and H_2O^+ Towards W49N: A Probe of Diffuse Clouds with a Small Molecular Fraction. *Astron. Astrophys.* **2010**, *521*, No. L10.
(21) Schilke, P.; Comito, C.; Müller, H. S. P.; Bergin, E. A.; Herbst, E.; Lis, D. C.; Neufeld, D. A.; Phillips, T. G.; Bell, T. A.; Blake, G. A.; et al. Herschel Observations of Ortho- and Para-Oxidaniumyl(H_2O^+) in Spiral Arm Clouds Toward Sagittarius B2(M). *Astron. Astrophys.* **2010**, *521*, No. L11.
(22) Lis, D. C.; Phillips, T. G.; Goldsmith, P. F.; Neufeld, D. A.; Herbst, E.; Comito, C.; Schilke, P.; Müller, H. S. P.; Bergin, E. A.; Gerin, M.; et al. Herschel/HIFI Measurements of the Ortho/Para Ratio in Water Towards Sagittarius B2(M) and W31C. *Astron. Astrophys.* **2010**, *521*, No. L26.
(23) Heisenberg, W. Mehrkörperproblem und Resonanz in der Quantenmechanik. *Z. Phys.* **1926**, *38*, 411−426.
(24) Dirac, P. A. M. On the Theory of Quantum Mechanics. *Proc. R. Soc. London* **1926**, *A112*, 661−677.
(25) Tomonaga, S. *The Story of Spin*; University of Chicago Press: Chicago, IL, 1973.
(26) Oka, T. The Parity of Rotational Levels. *J. Mol. Spectrosc.* **1973**, *48*, 503−507.
(27) Steimle, T. C.; Brown, J. M.; Curl, R. F., Jr. Microwave Optical Double Resonance of NH_2. VI. Ground State of NHD. *J. Chem. Phys.* **1980**, *73*, 2552−2558.
(28) Feller, D.; Davidson, E. R. *Ab Initio* Configuration Interaction Calculations of the Hyperfine Structure in Small Radicals. *J. Chem. Phys.* **1984**, *80*, 1006−1017.
(29) Weis, B.; Carter, S.; Rosmus, P.; Werner, H. J.; Knowles, P. J. A Theoretical Rotationally Resolved Infrared Spectrum for $H_2O^+(X^2B_1)$. *J. Chem. Phys.* **1989**, *91*, 2818−2833.
(30) Staikova, M.; Engels, B.; Peric, M.; Peyerimhoff, S. D. *Ab Initio* Calculations of the Vibrationally Averaged Hyperfine Coupling Constants in the $1^2\Pi_u(X^2B_1,A^2A_1)$ State of the Water Cation. *Mol. Phys.* **1993**, *80*, 1485−1497.
(31) Nakatsuji, H.; Ehara, M.; Momose, T. Hyperfine Splitting Constants Studied by the Symmetry Adapted Cluster-Configuration Interaction Method. *J. Chem. Phys.* **1994**, *100*, 5821−5828.
(32) Lushington, G. H.; Grein, F. Multireference Configuration Interaction Calculations of Electronic *g*-Tensors for NO_2, H_2O^+, and CO^+. *J. Chem. Phys.* **1997**, *106*, 3292−3300.
(33) Mürt, P.; Zink, L. R.; Evenson, K. M.; Brown, J. M. Measurement of High-Frequency Rotational Transitions of H_2O^+ in its Ground State by Far-Infrared Laser Magnetic Resonance (LMR) Spectroscopy. *J. Chem. Phys.* **1998**, *109*, 9744−9752.
(34) Dirac, P. M. A. The Quantum Theory of the Emission and Absorption of Radiation. *Proc. R. Soc. London* **1927**, *A114*, 243−265.
(35) Oka, T.; Welty, D. E.; Johnson, S.; York, D. G.; Dahlstrom, J.; Hobbs, L. M. Anomalous Diffuse Interstellar Bands in the Spectrum of Herschel 36. II. Analysis of Radiatively Excited CH^+, CH, and DIBs. *Astrophys. J.* **2013**, in press.
(36) Anicich, V. G.; Huntress, W. T., Jr. A Survey of Bimolecular Ion−Molecule Reactions for Use in Modeling the Chemistry of Planetary Atmospheres, Cometary Comae, and Interstellar Clouds. *Astrophys. J. Suppl.* **1986**, *62*, 553−672.
(37) Honvault, P.; Jorfi, M.; Gonzalez-Lezana, T.; Faure, A.; Pagani, L. *Ortho-Para* H_2 Conversion by Proton Exchange at Low Temperature: An Accurate Quantum Mechanical Study. *Phys. Rev. Lett.* **2011**, *107*, No. 023201.
(38) Crabtree, K. N.; McCall, B. J. The Ortho:Para Ratio of H_3^+ in Laboratory and Astrophysical Plasmas. *Philos. Trans. R. Soc.* **2012**, *A370*, 5055−5065.
(39) Schilke, P. Private communication.
(40) Oka, T.; Shimizu, F. O.; Shimizu, T.; Watson, J. K. G. Possible Rotational Equilibration of Interstellar Ammonia by Radiative $\Delta k = \pm 3$ Transitions. *Astrophys. J.* **1971**, *165*, No. L15.
(41) Oka, T.; Epp, E. The Nonthermal Rotational Distribution of H_3^+. *Astrophys. J.* **2004**, *613*, 349−354.
(42) Oka, T.; Geballe, T. R.; Goto, M.; Usuda, T.; McCall, B. J. Hot and Diffuse Clouds Near the Galactic Center Probed by Metastable H_3^+. *Astrophys. J.* **2005**, *632*, 882−893.
(43) Hirota, E. *High-Resolution Spectroscopy of Transient Molecules*; Springer-Verlag: Berlin, 1985; in Table 2.4.